6-1-2021

Manganese Oxide Carbon-Based Nanocomposite in Energy Storage Applications

Mulugeta Wayu

solids

MDPI

Review

Manganese Oxide Carbon-Based Nanocomposite in Energy Storage Applications

Mulugeta Wayu

Chemistry Department, Tennessee State University, 3500 John A Merritt Blvd, Nashville, TN 37209, USA; mwayu@tnstate.edu; Tel.: +1-615-963-5338

Abstract: Global increasing demand in the need of energy leads to the development of non-conven tional, high power energy sources. Supercapacitors (SCs) are one of the typical non-conventional energy storage devices which are based on the principle of electrochemical energy conversion. SCs are promising energy storage devices for better future energy technology. Increasing progress has been made in the development of applied and fundamental aspects of SCs. Manganese oxide electrode materials have been well studied; however, their capacitive performance is still inadequate for practical applications. Recent research is mainly focused on enhancing manganese oxide capacitive performance through the incorporation of electrically conductive materials and by controlling its morphology to reveal a more active surface area for redox reactions. In this review, progress in the applications of manganese oxide carbon-based materials towards the development of highly effective SCs is briefly discussed. In this regard, manganese oxide carbon-based nanocomposites synthesis methods and techniques used to approximate the capacitance of electrode materials are discussed.

Keywords: manganese oxide; carbon-based composites; electrochemical capacitors; supercapacitors energy storage; nanostructures

Citation: Wayu, M. Manganese Oxide Carbon-Based Nanocomposite in Energy Storage Applications. *Solids* **2021**, *2*, 232–248. https://doi.org/10.3390/solids2020015

Academic Editors: Vivek Kumar and Charles C. Chusuei

Received: 24 April 2021
Accepted: 17 May 2021
Published: 1 June 2021

1. Introduction

The global energy demand is rising with population growth and improved standards of living [1]. The advance in technology, the fast growth of portable electronic devices, and hybrid electric vehicles added to the urgent and increasing need for sustainable and renewable high-power energy sources. Today, most of our energy needs are met by fossil fuels. The use of fossil fuels as an energy source is causing environmental concerns, particularly global warming, and the emission of toxic chemicals [2]. To address this problem, the development of alternative energy storage/conversion devices with high power and high energy densities is crucial. Thus, renewable and sustainable energy sources are being extensively pursued [1,3,4].

Batteries, the most common electrical energy storage device, provide a suitable level of power for numerous applications and needs of everyday life. Even though batteries store a high amount of energy in a relatively small mass and volume, their slow power delivery, as illustrated in a Ragone plot (Figure 1), is a challenge [4,5]. Thus, their application is hindered in systems where fast storage with high power is needed. On the other hand, owing to their higher power density, excellent durability, and fast charge-discharge processes, electrochemical capacitors (ECs), or supercapacitors (SCs) have drawn tremendous attention as an alternative or supplement to batteries in energy storage systems [1,3,6–8]. Both batteries and ECs standalone technologies lack the essential merits to meet the commercial needs already established by fossil fuel consumption. To tackle these challenges, numerous efforts have been made to combine high power density SCs with high energy density batteries to form hybrid SCs (Figure 1) [1,4]. However, increasing the energy density of SCs to approach that of batteries, or enhancing the power density of batteries to reach that of SCs, comes at the cost of losses in the power of SCs and deteriorations in the energy of batteries [4,9,10].

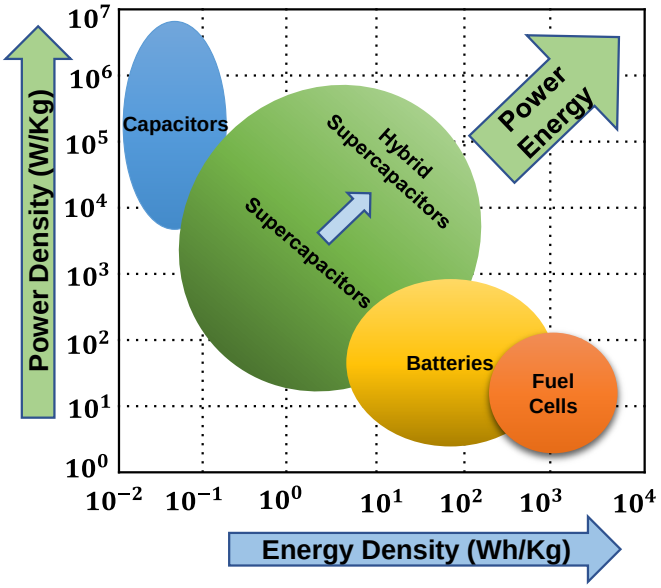

Figure 1. Ragone plot of the power–energy density range for various electrochemical energy storage devices.

Depending on their energy storage mechanisms, ECs are categorized into the electrical double layer (EDL), the redox capacitors, aka faradaic pseudo-capacitors, and hybrid capacitors [1,11,12] (Figure 2A). The EDL capacitors store energy by charge separation formed at the interface between the electrode and the electrolyte. During the charging process, the positive surface of EDL capacitors attracts the anions of electrolytes, while the cations accumulate on the negative electrode surfaces (Figure 2B). The EDL capacitance depends on the specific surface area of the electrode, the type of electrolyte, and the effective thickness of the double layer (the Debye length) (Equation (1)) [5].

$$C_{dl} = \frac{\varepsilon_\tau \varepsilon_0 A}{d} \quad (1)$$

where C_{dl} is the capacitance of the EDL, ε_τ is the electrolyte dielectric constant, ε_0 is the dielectric constant of the vacuum, d is the effective thickness of the double layer, and A is the electrode surface area. Since only ions which are accessible to the electrode surface contribute to the capacitance, optimization of surface properties and conductivities of the electrode materials are necessary for the development of improved ECs.

The development of improved SCs depends on the discovery of new electrode materials as well as a clear understanding of active ions in the electrolyte. Carbon-based materials were first employed in the ECs by Becker in 1957 [5]. Since then, numerous carbon-based materials with various components and structures have been synthesized and applied as ECs. For most EDL capacitors, carbon-based materials with a high surface area were frequently employed as electrode materials. These materials include activated carbon, carbon nanotubes, graphene, mesoporous carbon, and carbon-fiber-based materials, etc. [1,6,13,14]. Among these carbon-based materials, owing to their high specific surface area and long-term conductivity, single-layered graphene, and multiwalled carbon nanotubes attracted much research attention [1,15–17]. However, due to the difficulties in controlling pores size, active surface area, and surface chemistry of such electrodes, it is very challenging to increase the specific and/or volumetric capacitances. In the effort to enhance the energy densities of carbon-based ECs, metal oxides that undergo fast surface redox (pseudocapacitive) reactions were explored and incorporated [8,12,17–20].

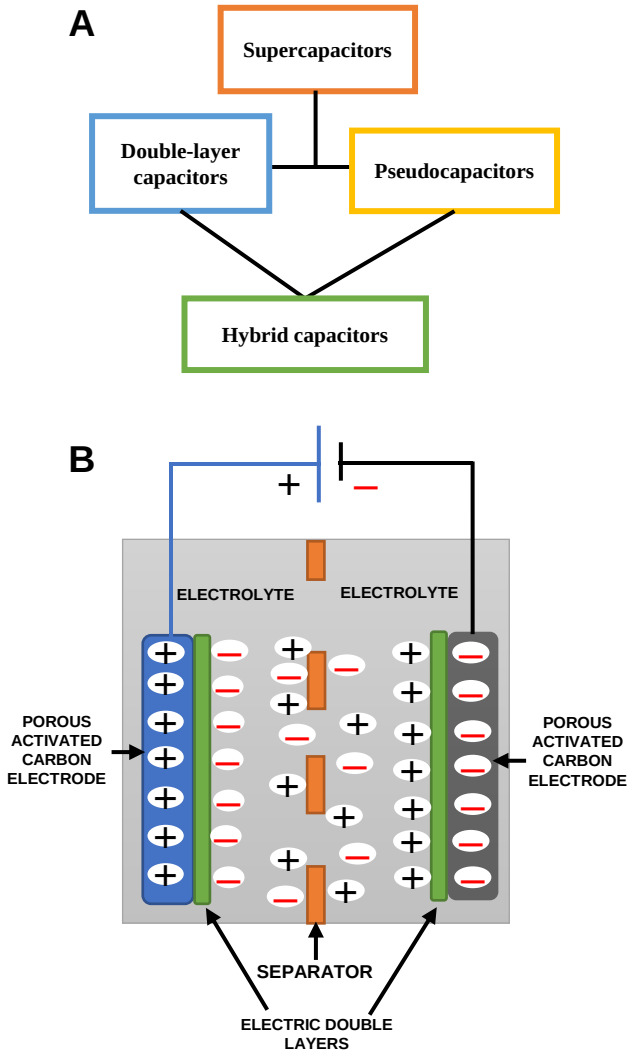

Figure 2. Schematic of (**A**) types of supercapacitors and (**B**) electrical double layer.

In the faradaic pseudo-capacitors, the energy is mainly stored by a fast and reversible faradaic redox reaction on the solid electrode surface, formed with electroactive materials in the electrolyte. Charges accumulated in the pseudo-capacitor are strongly related to the electrode potential (Equation (2)).

$$C = \frac{dQ}{dV} \tag{2}$$

where C is the capacitance of the faradic pseudo-capacitor, Q is the quantity of charge, and V is the potential. Unlike EDL, faradic pseudo-capacitors offer higher capacitance. However, they suffer from low power density, poor electrical conductivity, and lack of stability due to framework inflating during cycling. Significant efforts were made to find alternative, new, and cheaper materials. Certain transition metal oxides and/or conducting polymers with high capacitance were identified and applied as the electrode materials in faradaic pseudo-capacitors [1,4,6,12,21]. To enhance ECs, the various research trends either prepare composite electrodes by coating thin films of metal oxides or by coating conducting polymers on substrates with high surface area, such as carbon nanotubes, which additionally presents a high double-layer capacitance [4,14,21].

Amorphous hydrated ruthenium oxide (RuO_2) has been known to exhibit an ideal pseudocapacitive property, noticeably high specific capacitance, excellent reversibility in a wide potential range, and much longer cycle life. Many literature reviews show that the incorporation of RuO_2 significantly improved the specific capacitance of carbon-based materials [22–25]. For example, Yang et al. [26] prepared a hybrid nanostructure of

hydrous RuO_2 nanoparticles deposited on the surface of SWCNT/graphene composite via a sol–gel process and low-temperature annealing and obtained a specific capacitance of 988 F/g. Chen et al. [27] have obtained ultrahigh specific capacitance (1500 F/g) by constructing 3D-RuO_2-nanoporous gold hybrid composites. Das et al. [16] reported a specific capacitance up to 1084 F/g for electro-deposited RuO_2 onto high porous SWCNT films. The specific capacitance for the RuO_2 alone, calculated from the 2.5X porous film, was 1715 F/g, which is close to the estimated theoretical maximum value (2000 F/g). Despite the excellent performance, due to the high cost and toxicity, RuO_2's practical application is limited [3,6,14,28]. Alternatively, manganese oxide is gaining tremendous research attention as an active ECs electrode material. In this review, progress in manganese oxide (Section 2) and its carbon-based nanocomposite materials (Section 3) application towards the development of improved ECs is briefly discussed. A few figures from selected papers are presented and briefly illustrated for better insights.

2. Manganese Oxide

The application of Manganese oxide (denoted as MnO_x hereafter) in SCs was first reported in 1999 [21,29]. Since then, MnO_x has been widely studied as an active, low-cost, and biofriendly ECs material [8,21,29,30]. Why are manganese or its oxides are so appealing for SCs applications? First, manganese is a transition metal with five unpaired electrons, which possesses the most oxidation states, including the highest oxidation state (VII) in the entire periodic table [31]. Due to its unique electronic structure, manganese is extremely redox-active, thus, it exists in several oxide forms (including MnO, MnO_2, Mn_2O_3, Mn_3O_4 ($MnO.Mn_2O_3$), and Mn_2O_7). Second, Manganese is the most abundant transition metal among oxides which are pseudocapacitive. Third, MnO_x exhibits high theoretical capacitance (1370 F/g for MnO_2 for instance) with a wide positive potential window compared to other transition metal oxides [31,32]. MnO_x offers outstanding electrochemical behavior, environmental compatibility, and excellent structural multiformity, combined with novel chemical and physical properties [1,3,5–8,11–13,30–33].

The pseudocapacitance of MnO_x electrodes arises from the redox reactions of the oxide with ions in the electrolyte solution. Since manganese has several oxidation states, there are plenty of opportunities for redox reactions involving the ion exchange between MnO_x and electrolytes, and between oxidation state transitions (such as Mn (III)/Mn (II), Mn (IV)/Mn (III), and Mn (VI)/Mn (IV)) [21,33]. How the charges are stored is still a question. According to recent studies, charge storages by MnO_x electrodes are influenced by several factors, such as the bandgap, point of zero charges, tunnel sizes of the electrode material, work function, pH, and stability window of the electrolyte. The detailed charge storage mechanism is still being studied using various techniques [21].

Various nanostructures of MnO_x with improved electrical conductivity, novel morphology, high surface area, and controlled pore sizes were developed, and their specific capacitances were studied [21,34–41]. For instance, nanostructured MnO_2 was prepared via the sonochemistry method and yielded a specific capacitance of 344 F/g [6]. The specific capacitance was significantly affected by the crystal structure of the electrode material. Wei et al. [30] anodically electro-deposited MnO_2 nanocrystals with three types of crystal structures, i.e., ε-MnO_2 (Figure 3A), rock salt-MnO_2 (Figure 3B), and antifluorite-MnO_2 (Figure 3C), by introducing complexing agents such as EDTA disodium salt and sodium citrate salt. As illustrated in Figure 3D, the capacitive performance of the MnO_2 nanocrystals depends strongly on their crystal structures. Antifluorite-MnO_2, which has a morphology with few surface areas and similar chemistry compared to rock salt-MnO_2 and ε-MnO_2, showed superior capacitive behavior. This behavior of antifluorite-MnO_2 relies on its crystal structure and defect chemistry. Defective antifluorite-MnO_2 has a cubic structure, which is less close-packed than the other two crystal structures. Defective antifluorite-MnO_2 possesses more octahedral vacancies than rock salt-MnO_2. The underlying cause for the superior capacitive performance of defective antifluorite-MnO_2 may be the presence

of more octahedral vacancies with a lower energy barrier, which allows faster intercalation/deintercalation of cations such as Na^+ during the charging-discharging process.

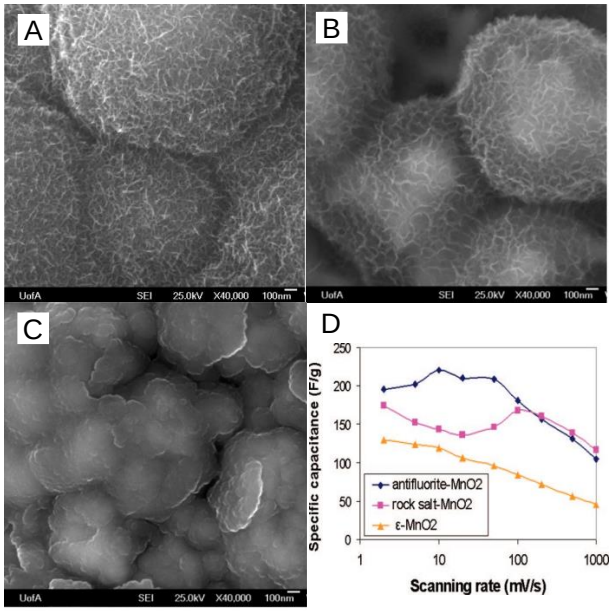

Figure 3. Morphology and crystal structure of manganese oxide prepared from 0.3 M $MnSO_4$ solution: SE image of (**A**) without any complexing agents, (**B**) with 0.2 M EDTA, (**C**) with 0.3 M sodium citrate, and (**D**) Specific capacitance of MnO_2 nanocrystals derived from the cyclic voltammograms (second cycle) at various cycling rates. Reproduced with permission from reference [30]. Copyright ©2008, American Chemical Society.

Based on a 1-electron redox reaction per manganese atom, the theoretical specific capacitance of MnO_2 was estimated to be 1370 F/g [8,20,38,42]. Such a maximum value can only be achieved using ultrathin films of MnO_2. Moreover, due to the high ion/charge transfer resistance and poor conductivity of pure MnO_2, the release and utilization of its high theoretical capacitance are difficult [20,21,43]. To obtain an improved SC, significant efforts were made to combine pseudocapacitive MnO_x with an electrically conductive substrate or supportive backbones [21]. In Section 3 of this review, applications of hybrid electrodes, comprising MnO_x, electrically conductive components, and carbon-based materials as the supportive backbone for the development of improved supercapacitors are briefly explained.

3. Carbon-Based Material/MnO_x Composite

Carbon-based materials and MnO_x alone have been investigated for ECs use [21,36,44–48]. Carbon-based materials, in various forms and textures, have a high specific surface area and outstanding electrical conductivity [49,50]. MnO_x, although suffering from poor electrical conductivity and less tunable specific surface area, displays higher ECs compared to carbon-based materials [6,51]. By combining these two materials while maintaining their merits and/or with generated synergistic effects, many papers are emerging showing improved specific capacitance [21,52]. In the hybrid electrode, carbon-based materials are used as a supporting backbone and exposed large specific surface area for MnO_x deposition, enhanced electrical conductivity, increased mechanical strength, and provide channels for fast charge transport, while MnO_x is responsible for the charge storage [20–22,52]. To obtain the optimum electrochemical performance from the hybrid materials, controlling their physical properties, composition, structural feature, and morphology along with their interfaces is of crucial importance. In this section, we briefly discussed the applications of various carbon-based materials/MnO_x composites for the development of better specific capacitive SCs.

3.1. Activated Carbon/MnOx Composite

Activated carbon (AC) is a form of carbon with small, low-volume pores that increase its surface area. Due to these outstanding properties, AC has been used as a support for metal oxides, such as MnO_2, in ECs applications. For instance, Huang et al. [2] fabricated a porous nano-MnO_2 decorated bamboo-based AC through an in situ preparation method and reported a specific capacitance of 221.45 F/g at the current density of 1 A/g. The specific capacitance was enhanced by the synergistic effect of the two components, i.e., the bamboo-based AC displayed an extraordinary 3D microstructure and high absorptive capacity, while the nano-sized MnO_2 with a large surface area offered many sites for the redox reaction. Jang et al. [53] combined AC and MnO_2 to form AC/MnO_2 hybrid electrode. MnO_2 was deposited on the AC electrode surface by dipping the electrode into an aqueous solution of permanganate. The as-prepared hybrid electrode yielded a specific capacitance of 290 F/g. Controlled urchin type MnO_2 microspheres were electro-deposited on the conductive graphene/AC composite to obtain a 3D graphene/AC/MnO_2 flexible electrode, which resulted in a high area-specific capacitance [54] (Figure 4). As illustrated in Figure 4A, graphene/AC/MnO_2 composite electrodes were prepared in two steps: (i) AC particles were bonded to graphene 2D sheets using self-assembly method by vacuum filtration, and (ii) MnO_2 nanostructures were electro-deposited on graphene/AC working electrodes at various reaction times. The high-magnification FE-SEM images of graphene/AC/MnO_2 prepared at 1200 s reaction time were displayed in Figure 4B–D. The TEM image of graphene/AC/MnO_2-1200 s was shown in Figure 4E. MnO_2 microspheres were uniformly dispersed in flexible graphene/AC substrate. The area-specific capacitances of the electrodes were displayed in Figure 4F. Graphene/AC/MnO_2-1200 s showed the highest area-specific capacitance (1231 mF/cm^2). This high capacitance is due to the synergistic effects among the graphene, porous AC, and high theoretical capacitive MnO_2. The electro-deposition reaction time played a great role in controlling the morphology of MnO_2 microspheres, and hence, the ECs performance of the electrodes. The results suggest the broad future applications of the composites in flexible and wearable electronics.

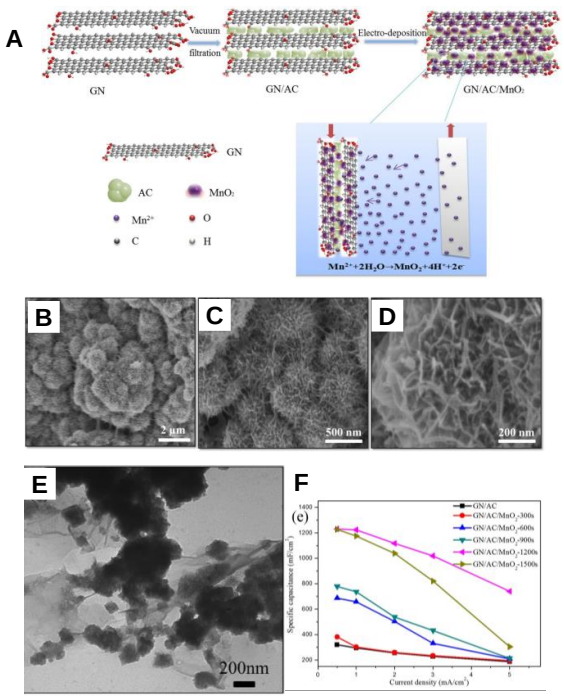

Figure 4. (**A**) Schematic illustrations for the preparation process of GN/AC/MnO_2 composite electrodes, (**B**–**D**) GN/AC/MnO_2-1200 s composite films at high magnifications, (**E**) TEM image of GN/AC/MnO_2-1200 s composite films, and (**F**) specific capacitances of electrodes at various current densities. Reproduced with permission from reference [54]. Copyright ©2017, The Author(s).

Wang et al. [51] synthesized a MnO_2/AC composite with high electrochemical performance via a grafting oxidation method, which resulted in a specific capacitance of up to 332.6 F/g at a scanning rate of 2 mV/s. Qiu et al. [35] electro-deposited MnO_2 over AC paper (ACP) to form MnO_2/ACP composite. The as-prepared composite showed an excellent capacitive performance (specific capacitance of 485.5 F/g, calculated from discharge curve with a current density of 2.0 A/g). Cheng et al. [55] prepared a MnO_2/ACP composite by activating commercial carbon paper (ACP) using potassium dichromate lotion and then anchored MnO_2 nanoribbons onto ACP via an electro-deposition route. A specific capacity as high as 757.0 F/g was obtained. This high specific capacitance was probably due to the enlarged specific area and improved electronic conductivity of the as-prepared composite. All the studies suggest that MnO_2 integrated with AC is a promising electrode material for the development of efficient SCs.

3.2. Carbon Nanotubes/MnOx Composite

Since its discovery by Iijima in 1991 [56], carbon nanotubes (CNT) have been extensively investigated. CNT comes in various forms, the most dominant being single-walled (SWNT) and multi-walled nanotubes (MWNT). Due to their excellent mechanical property, good electrical conductivity, unique pore structure, and chemical stability, carbon nanotubes have been applied in ECs as electrode materials [18,45,57–70]. The specific capacitance of CNT electrodes that have been reported is relatively lower than that of an AC electrode with a larger surface area [11]. To enhance its capacitance, CNT has been combined with MnO_x to form CNT/MnO_x composite for SCs applications. For instance, Lee et al. [8] reported LbL-MWNT/MnO_2 ultrathin film electrodes through a layer-by-layer (LbL) assembly of functionalized MWNTs and continuous redox deposition of MnO_2 onto MWNTs. As noted above, the MWNT network created fast electronic and ionic conducting channels in the presence of an electrolyte, and the coatings of MnO_2 on the network provided high volumetric capacitance (246 F/cm^3). Hou et al. [60] constructed a ternary nanocomposite film comprising of MnO_2, CNT, and a conducting polymer (Figure 5A). Functionalized few-walled CNT (fFWNTs) (Figure 5B) were ultrasonically mixed with MnO_2 precursors to form the hierarchical MnO_2 nanosphere (Figure 5C) on the CNT network. MnO_2 loadings on fFWNTs were controlled by varying the ratio of the two components.

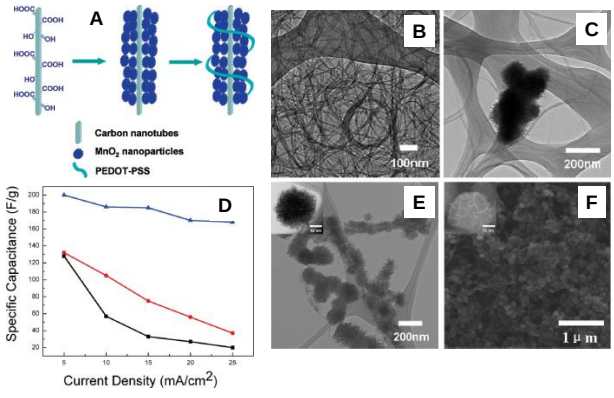

Figure 5. (**A**) Sketch of MnO_2/CNTs/PEDOT-PSS ternary composite formation; (**B**) TEM image of fFWNTs, (**C**) TEM image of direct mixing of MnO_2 nanospheres with fFWNTs, and (**E**) TEM and (**F**) SEM images of PEDOT-PSS dispersed MnO2 nanospheres in situ grown on fFWNTs; (**D**) Specific capacitance of MnO_2/fFWNT/PEDOT-PSS ternary composite (blue), MnO_2/PEDOT-PSS composite (red), and MnO_2 film (black) at different charge/discharge current densities. Reproduced with permission from Reference [60]. Copyright ©2010, American Chemical Society.

The morphology and microstructure of a sample composite, which comprises of conducting polymer is depicted in Figure 5E,F. The MnO_2 nanospheres have uniform "crumpled paper ball" morphology (Figure 5E inset) with small "wormhole-like" pores

(Figure 5F inset). Although a unique hierarchical MnO_2 with no aggregations was grown on a continuous fFWNTs network, the exact growth mechanism is not yet completely understood. The electrochemical performance of the nanocomposite film, evaluated by cyclic voltammetry, yielded a specific capacitance of up to 200 F/g (Figure 5D). It was noticed that the individual components of the film greatly contributed to the enhancement of the specific capacitance. Wang's group [20] synthesized a superior supercapacitor nanocomposite based on porous CNTs, i.e., MnO_2/PCNTs/MnO_2. The nanocomposite displayed a specific capacitance as high as 341.5 F/g at 2 mV/s and 214.3 F/g at 100 mV/s. This high capacitance was due to the presence of massive nanopores on the walls of PCNTs (6 nm), which led to the loadings of a large amount of MnO_2 nanoparticles (2.42 nm), both in the nanocavity and on the surface of PCNTs as electroactive sites. The results imply a new designing strategy for supercapacitor materials with outstanding performance. Qian et al. [71] synthesized aqueous inorganic ink comprised of hexagonal MnO_2 nanosheets using a simple chemical reduction method. A flexible electrode for capacitive energy storage was obtained by printing the MnO_2 ink onto commercially available A4 paper, which was pretreated with MWCNT. The as-prepared electrode yielded a maximum specific capacitance of up to 1035 F/g. This high capacitive property of MnO_2 ink sets a stage for its candidacy for the large-scale production of high-performance SCs in the future.

3.3. Carbon Spheres/MnO_x Composite

The use of carbon spheres (CS) in ECs and capacitive flowable suspension electrodes was investigated [19,72,73]. Active materials with a spherical morphology are highly desired in flowable electrodes. CS with small diameters are a potential candidate for better ECs performance, owing to their highly accessible surface area and excellent flow characteristics. To date, only a few papers reported the preparation of low-sized CS and tested for capacitive flowable electrodes. Zhang's group prepared highly porous monodispersed CS with a very high specific surface area (2900 m^2/g) and narrow pore size distribution (<3 nm) and reported a specific capacitance of 168 F/g. The CS was synthesized using emulsion polymerization of resorcinol-formaldehyde, followed by carbonization and CO_2 activation [73]. The mass loading of MnO_x and capacitive performance is dependent on the size of the CS. Small-sized CS was preferred, to obtain MnO_x/CS with a high specific surface area. Wang's group hydrothermally coated carbon microspheres (≈1 μm diameter) with a whisker-like MnO_2 and maintained a relatively high surface area (142.46 m^2/g). The as-prepared MnO_2/CS composite yielded a capacitance of about 180 F/g at a current density of 1 A/g for the charge/discharge measurements [42]. However, when CS with a smaller diameter was used, the MnO_2/CS composite surface area was much higher (269.2 m^2/g) (Figure 6). The resulting specific capacitance of MnO_2/CS was 252 F/g (at a sweep rate of 2 mV/s for CV measurement) [74]. Here, a facile, cost-effective preparation method was used to create Carbon@MnO_2 core-shell hybrid nanospheres for supercapacitor electrode materials. The schematic of the preparation process is depicted in Figure 6A. The bare CS with smooth surfaces was not aggregated (Figure 6B). This property led to the formation of a uniform flower-like MnO_2 shell anchored on CS surfaces. As noticed in Figure 6C,D, the thickness of the MnO_2 shell is also uniform on CS surfaces. The lattice spacing indicated the crystalline structure of the shell was δ-MnO_2 (Figure 6D inset).

Yang et al. [75] developed a facile soft templating strategy for the synthesis of hollow spheres of nanocarbon by hydrothermal process. Then permanganate (MnO_4^-) was incorporated into the hollow CS to grow nanocrystalline MnO_2 on the carbon surface, resulting in the hollow carbon-MnO_2 hybrid particles. Xiong et al. [76] fabricated novel honeycomb MnO_2 nanospheres/carbon nanoparticles/graphene (MnO_2/C/G) composites by freeze-drying method. The carbon nanoparticles in the composite effectively prevented graphene from restacking and agglomeration while MnO_2 nanospheres were dispersed on the graphene surface (Figure 7). As depicted in Figure 7a,b, MnO_2 nanospheres with a honeycomb-like structure and size of about 100 nm are formed by the self-assembly of MnO_2 nanoplatelets. The images of the MnO_2/C/G composite (Figure 7c,d) revealed that

the honeycomb MnO_2 nanospheres were covered by wrinkled and transparent graphene (G) (indicated by red arrows) with few exposed surfaces. Carbon nanoparticles (C) in the composite were not observed in the images, as they are probably covered by graphene. However, their presence in the composite was revealed by EDX (Figure 7e). TEM images (Figure 7f) of the composites clearly showed the presence of graphene (wrinkled and folded), honeycomb MnO_2 (green rounds), and carbon nanoparticles (blue rounds). MnO_2 and carbon nanoparticles were well dispersed on graphene surfaces without forming aggregation. As a result, the composite showed an improved specific capacitive property (255 F/g at a current density of 0.5 A/g).

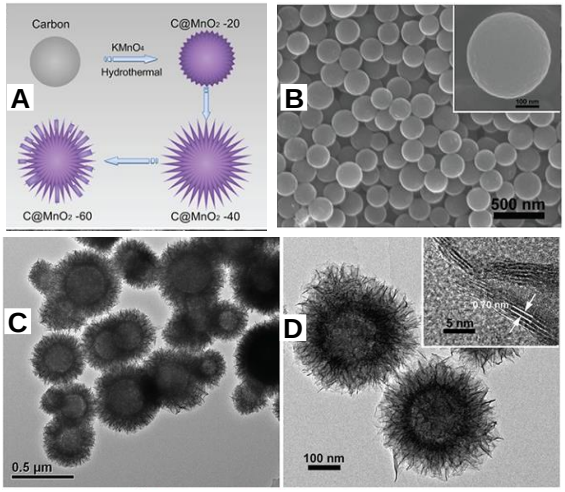

Figure 6. (**A**) Schematic illustration of the fabrication process of the carbon@MnO_2 nanospheres. (**B**) SEM images of bare carbon nanospheres. (**C**,**D**) Typical TEM images of carbon@MnO_2 at different magnifications; inset of (**D**) is the HRTEM image of a MnO_2 nanosheet. Reproduced with permission from [74]. Copyright ©2014, Elsevier B.V.

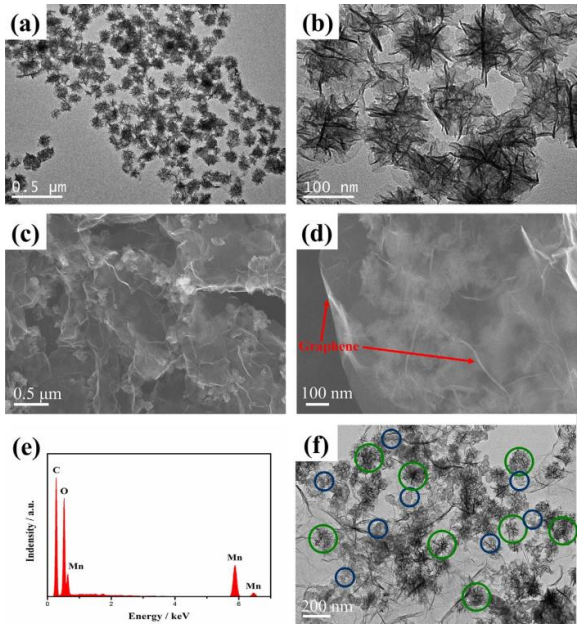

Figure 7. (**a**,**b**) TEM images of honeycomb MnO_2 nanospheres; (**c**,**d**) FE-SEM images of MnO_2/C/G composites; (**e**) EDX spectrum of MnO_2/C/G composites; (**f**) TEM image of MnO_2/C/G composites. Reproduced by permission from [76]. Copyright ©2015, Elsevier B.V.

Ranjusha et al. [77] presented the synthesis of carbonized MnO_2 nanowires, using carbon nanobeads to fabricate a rechargeable electrode with a large surface area, high power, and energy density for supercapacitor or battery applications. The electrodes showed a specific capacitance as high as 1200 F/g. The high surface area and conductivity of the materials contributed to the enhancement of mass-specific capacity. The practical application of the thin films, tested in a working model of a button cell, exhibited a capacitance of about 1.2 F/g, an energy density of 96 Wh/kg, and a peak power density of 32 kW/kg, suggesting the future potential application of such electrodes.

3.4. Carbon Nanofibers/MnO_x Composite

Fiber-based SCs have drawn tremendous attention due to their very low volume, high flexibility, and weave-ability of the fibers, which are desired for the development of high-performance electrodes. Carbon nanofibers (CNFs) have been applied as support for MnO_x [78–80]. CNFs with a smaller diameter are desired for higher loading of MnO_x. For instance, Zhang et al. [58] reported the design and fabrication of hierarchically structured MnO_2/graphene/CF and studied its practical application in SCs. Wang et al. [81] demonstrated the construction of a novel high-performance asymmetric supercapacitor based on freestanding MnO_2/CNF hierarchical composites and activated carbon nanofibers (ACNF) as the (+) and (−) electrodes, respectively, in an aqueous electrolyte solution of Na_2SO_4 (Figure 8). The electrochemical measurements indicated that the as-prepared supercapacitor can yield a specific capacitance as high as 56.8 F/g, with a high energy density of 30.6 Wh/kg at a power density of 200 W/kg. The results suggest an effective and convenient route for the construction of asymmetric SCs based on freestanding electrode materials for high-energy and high-power density systems.

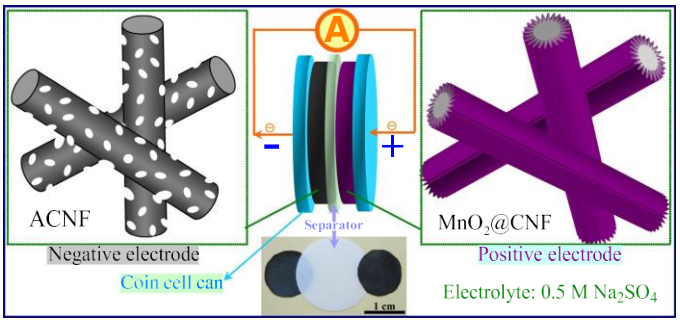

Figure 8. Illustration of the as-assembled asymmetric supercapacitor cell with MnO_2/CNF composite as positive electrode and ACNF as a negative electrode in mild Na_2SO_4 aqueous electrolyte. Reproduced with permission from [81]. Copyright ©2013, Elsevier Ltd.

Bao et al. [82] demonstrated the design and fabrication of a novel flexible nanoarchitecture by a facile coating of ultrathin MnO_2 films onto highly electrically conductive Zn_2SnO_4 nanowires grown radially on carbon microfibers (CMFs) to achieve high specific capacitance, high-energy density, and long-term life for supercapacitor electrode applications. A specific capacitance of up to 642.4 F/g was observed. Xu et al. [83] designed and fabricated a flexible asymmetric supercapacitor (ASC) with high energy density using flower-like Bi_2O_3 and MnO_2 grown on carbon nanofiber (CNF) paper. Chen et al. [84] fabricated nanoflake MnO_2@Carbon fiber-coaxial nano cables by a facile electrochemical deposition-oxidation route. The as-prepared material, when used as an electrode, resulted in a specific capacitance of up to 511.8 F/g. Dang et al. [85] reported self-grown MnO_2 on carbon fiber paper via a facile redox reaction, which was constructed by an interconnected ultrathin nanosheets array. The CFP acted as both a supporting scaffold and a reducing agent for MnO_2 growth. The as-prepared MnO_2/CFP composite, when used as an electrode material, resulted in a specific capacitance of up to 713.7 F/g (0.5 A/g). A composite textile electrode with high specific capacitance (1516 mF/cm^2) was fabricated by introducing graphene/MnO_2 into activated carbon fiber felt (ACFF) [86].

3.5. Graphene/MnO_x Composite

Owing to their high specific surface area (SSA), graphene and CNT are frequently employed in hybrid electrodes. However, their practical application was hindered due to the presence of high contact resistance between graphene–graphene, CNT–CNT, or graphene–CNT. Besides, these electrodes suffer from the entanglement of CNT and the stacking of graphene. Recently many efforts have been made to combine MnO_x with CNTs and/or graphene to form ternary composites. Hybrid electrodes made of these composites showed higher specific capacitance and better cycle life compared to the individual components [87]. Yan et al. [7] synthesized a graphene–MnO_2 composite through the self-limiting deposition of nanoscale MnO_2 on the surface of graphene under microwave irradiation (Figure 9).

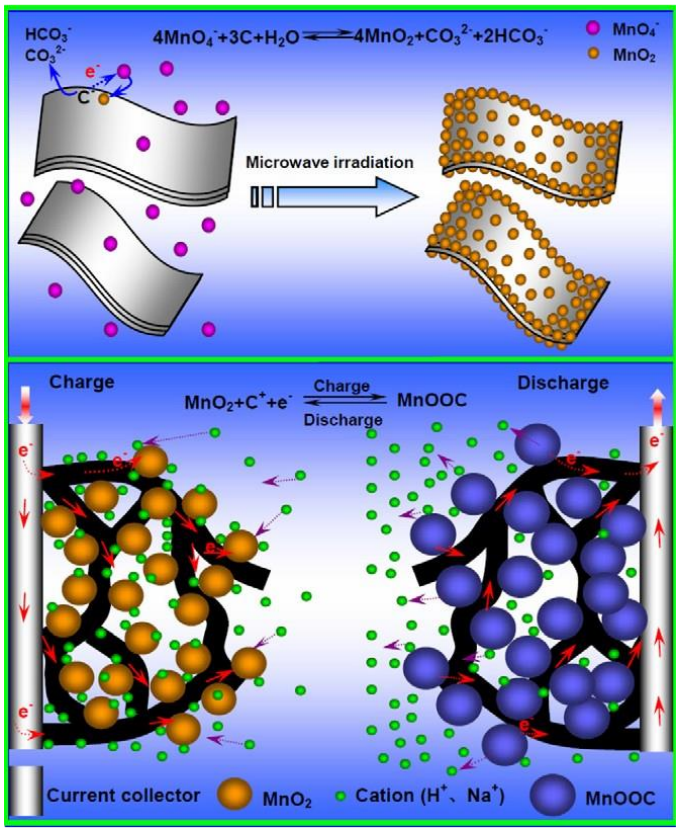

Figure 9. Schematic illustration for the synthesis and electrochemical performance of graphene–MnO_2 composite. Reproduced with permission from [5]. Copyright ©2000, Elsevier Science Ltd.

The as-synthesized nanostructured graphene–MnO2 hybrid materials were used to investigate the electrochemical behaviors. The graphene nanosheet in the composite provided conductive support and a large surface area for the deposition of nanostructured MnO_2. The graphene–MnO2 composite showed almost three times higher specific capacitance (310 F/g) than that of pure graphene (104 F/g) and birnessite-type MnO_2 (103 F/g). The increase in specific capacity of the graphene/MO_2 composite might be due to the excellent interfacial contact area between graphene and MnO_2, and the high electrical conductivity of graphene. Lo et al. [1] studied the effect of graphene-to-CNT ratio, Mn content, and polyvinylidene fluoride (PVDF) on the capacitive behavior. They confirmed the bonding between amorphous MnO_2 and graphene-based materials and explained its potential for a significant reduction of polymer binding content. Their work suggests a valuable building block for the future development of composite electrodes for SCs. Overall, the specific capacitance comparison of some of MnO_x/carbon-based materials are compiled in Table 1.

Table 1. Specific capacitance comparison of some of carbon-based/MnO_x composite.

Material	C/Fg^{-1}	PD (kW/kg)	ED (Wh/kg)	C (Retention Cycle)	Ref.
α-MnO_2	167	-	-	89% (350)	[3]
Layered Structure MnO_2	344 (5 mVs^{-1})	-	-	-	[6]
MnO_2 nanospheres	299	-	-	97.6% (1000)	[37]
MnO_2 nanoflower array	314	-	-	-	[38]
Bilayer MnO_x/Ni foam	559.5	-	-	-	[36]
α-MnO_x/CNTs/Ni	415 (5 mVs^{-1})			79% (1000)	[11]
MnO_2/GNS/CNT	367	-	-	83% (3000)	[87]
MnO_2/VACNTs	642 (10 mVs^{-1})	-	-	-	[70]
MnO_2/porous CNT/MnO_2	341.5 (2 mVs^{-1})			98% (6000)	[20]
Mixed nanocomposite (MWCNT/PPy: MnO_2)	365	-	44	-	[12]
Co-axial (MWCNT/Ppy/MnO_2)	270	-	36	-	[12]
MWCNT@MnO_2@Ppy	272.7	-	-	-	[46]
LbL-MWNT/MnO_2	** 246 (1000 mVs$^{-1)}$	-	-	-	[8]
Mn_xO_y/MWCNT hybrid	757	-	-	100% (10,000)	[62]
CNTs-MnO_2/rGO-PVDF	276.3	4.83	49.1	83% (1000)	[47]
δ-MnO_2/SWCNT	* 964	[a] 8.15 × 10^{-4}	[b] 3.18 × 10^{-5}	-	[64]
CNT/MnO_2 hybrid	300	[a] 2.5 × 10^{-3}	[b] 2.6 × 10^{-5}	-	[61]
MnO_2 nanosheets/MWCNT	1035	81	25.3	98.9% (10,000)	[71]
MnO_2/CNT/CP	200	-	-	>99% (1000)	[60]
Graphene-CNT/MnO_2	486.6	-	24.8	-	[68]
MnO_2/ACP	485.4	-	-	85% (2000)	[35]
Bamboo-Based AC@MnO_2	221.45 (5 mVs^{-1})			89.29% (1000)	[2]
AC/MnO_2	290	-	-	-	[53]
MnO_2/AC	332.6 (2 mVs^{-1})			99.99% (2000)	[51]
MnO_2/ACP	640.8 (10 mVs^{-1})	-	-	-	[55]
MnO_2@CS	150	9.627	8	74.4% (1000)	[19]
MnO_2/hollow CS	227.5	-	-	96% (5000)	[72]
Highly porous CS film	168	-	-	95% (5000)	[73]
MnO_2/CS	307.6	-	-	96.6% (1000)	[42]
Carbon@MnO_2 nanospheres	252 (2 mVs^{-1})	-	[bb] 3.7 × 10^{-4}	74% (2000)	[74]
MnO_2 NW/C nanobead	1200	32	96	-	[77]
CNP/MnO_2 nanorods	800 (5 mVs^{-1})	14	4.8	97.3% (10,000)	[79]
MnO_2/CNF	56.8	20.8	30.6	94% (5000)	[81]
Zn_2SnO_4/MnO_2/CMF	621.6 (2 mVs^{-1})	32	36.8	98.8% (1000)	[82]
Nanoflake MnO_2@CF	511.8 (2 mVs^{-1})	-	-	-	[84]
MnO_2/CFP	713.7	-	-	86.8% (1200)	[85]
Graphene/MnO_2	310 (2 mVs^{-1})	-	-	88% (15,000)	[7]
MnO_2/CNP/Graphene	255 (2 mVs^{-1})	-	-	83% (1000)	[76]
GR-MnO_2	274 (10 mVs^{-1})	0.225	23.9	96% (1000)	[88]
[RGO/MnO_2]$_{10}$	446 (5 mVs^{-1})	-	-	96% (1000)	[89]
Mn_3O_4/rGO	** 52.2	[aa] 0.018	[bb] 3.13	100% (10,000)	[48]
GN/AC/MnO_2	** 1231	[aa] 0.02	[bb] 2.7 × 10^{-4}	82.8% (10,000)	[54]
Graphene/MnO_2/ACFF	* 1.516	-	-	100% (5000)	[86]
N-rGO/CNT-MnO_2 film	418 (50 mVs^{-1})	12.526	45.72	-	[18]

Specific capacitance (C), Power density (PD), Energy density (ED), * the unit is Fcm^{-2}, ** the unit is Fcm^{-3}, [a] the unit is Wcm^{-2}, [aa] the unit is Wcm^{-3}, [b] the unit is Whcm^{-2}, [bb] the unit is Whcm^{-3}.

3.6. Other Materials/MnO_x Composite

Other MnO_x-based materials are also being studied for improved SCs. For example, Mahmood et al. [90] have reported high specific capacity by synthesizing ultrathin MnO_2 nanowire-intercalated 2D-MXenes. It was noted that the multiple redox sites provided by MnO_2 nanowire and high conductivity of MXene played synergistic roles to enhance the overall performance of the SCs. Ma et al. [91] used a simple liquid phase reaction method to prepare a stable MnO_2 nanowires@NiCo-layered double hydroxide (LDH). Uniform NiCo-LDH nanosheets were grown on an ultralong MnO_2 nanowires surface. They observed a specific capacitance as high as 708 F/g at 1 A/g. Sun et al. [92] applied oxidized carbon fibers as a support substrate for MnO_2 flowers-like sponge layer growth, followed by deposition of high-density grape-like Mn_3O_4 nanospheres, which expanded in the MnO_2 layer. The composite (MnO_2/Mn_3O_4) resulted in very high specific capacitance (1709 F/g at 1 A/g). Such study and results open a wide door of opportunities for the

preparation of hybrid carbon-based manganese oxide materials in a simple and tunable oxide nanostructure for future applications, not only in SCs, but in other areas such as electrocatalysis, lithium batteries, and wastewater treatments.

4. Summary and Future Perspective

Over the past two decades, the electrochemical performance of MnO_x-based supercapacitor electrodes has improved compared to earlier studies where MnO_x showed a specific capacitance of less than 200 F/g, with low retention at high current densities or scan rates [34,44,93]. Significant advances were achieved by investigating and incorporating carbon-based materials, which improved the accessible large surface area and active sites for redox reactions. Most MnO_x/carbon-based composites yielded a specific capacitance higher than 500 F/g [36,55,70,71,77,79,82,84,85]. However, only a few articles reported a specific capacitance higher than 1000 F/g [71,77].

This review briefly summarized the progress of the available structural designs for MnO_x/carbon-based materials in the ECs system. By careful assessment of various forms of carbon-based materials, the effect of size, structure, and morphology of the substrate on the capacitance of MnO_x/Carbon hybrid supercapacitor electrodes are shown. Of all the assessed nanostructures, ultrathin films of MnO_x with few nanometers thickness deposited on conductive substrates showed high specific capacitance (close to the theoretical values), due to the exposed electrochemically active sites of the substrates and the shortening of charge/electron transportation routes [41,43,71,77]. To attain these high capacitances, very low loading masses of MnO_2 are required, which are not practical yet. Extensive efforts are still needed to improve the electrochemical utilization of MnO_x, especially in cases where high mass loading is desired. For the overall performance of the ECs electrode, the choice and modification of the substrates and/or electrically conductive components are equally important. Besides, the selection of counter electrodes, current collectors, electrolytes, membrane separators, and handling/packaging of ECs cells need to be thoroughly examined.

Even though a significant effort has been made thus far, the full potential of MnO_x/carbon-based materials electrodes for SCs applications has not been realized. We are still far from achieving the theoretical capacitive values. However, as briefly outlined in the present review, a solid foundation for future technological advancements has been corroborated. It is anticipated that the above research findings might provide some technical insights to enhance the electrochemical performances of MnO_x/carbon-based materials [92]. Based on the wide applications of MnO_x and the scalability of carbon-based materials, it is believed that MnO_x/carbon-based hybrid electrodes offer promise for the development of high energy density with high power SCs.

Funding: The APC was funded by MDPI.

Data Availability Statement: Not applicable.

Acknowledgments: The author would like to thank the Tennessee State University Department of Chemistry for the opportunity and allotted time to write this review.

Conflicts of Interest: The author declares no conflict of interest.

References

1. Lo, A.Y.; Saravanan, L.; Tseng, C.M.; Wang, F.K.; Huang, J.T. Effect of Composition Ratios on the Performance of Graphene/Carbon Nanotube/Manganese Oxide Composites toward Supercapacitor Applications. *ACS Omega* **2019**, *5*, 578–587. [CrossRef]
2. Huang, T.; Zehai, Q.; Dewu, W.; Zhibiao, H. Bamboo-based activated carbon@ MnO_2 nanocomposites for flexible high-performance supercapacitor electrode materials. *Int. J. Electrochem. Sci.* **2015**, *10*, 6312–6323.
3. Xu, M.; Kong, L.; Zhou, W.; Li, H. Hydrothermal synthesis and pseudocapacitance properties of α-MnO_2 hollow spheres and hollow urchins. *J. Phys. Chem. C* **2007**, *111*, 19141–19147. [CrossRef]
4. Noori, A.; El-Kady, M.F.; Rahmanifar, M.S.; Kaner, R.B.; Mousavi, M.F. Towards establishing standard performance metrics for batteries, supercapacitors and beyond. *Chem. Soc. Rev.* **2019**, *48*, 1272–1341. [CrossRef] [PubMed]

5. Kötz, R.; Carlen, M. Principles and applications of electrochemical capacitors. *Electrochim. Acta* **2000**, *45*, 2483–2498. [CrossRef]
6. Zolfaghari, A.; Ataherian, F.; Ghaemi, M.; Gholami, A. Capacitive behavior of nanostructured MnO_2 prepared by sonochem-istry method. *Electrochim. Acta* **2007**, *52*, 2806–2814. [CrossRef]
7. Yan, J.; Fan, Z.; Wei, T.; Qian, W.; Zhang, M.; Wei, F. Fast and reversible surface redox reaction of graphene–MnO_2 composites as supercapacitor electrodes. *Carbon* **2010**, *48*, 3825–3833. [CrossRef]
8. Lee, S.W.; Kim, J.; Chen, S.; Hammond, P.T.; Shao-Horn, Y. Carbon Nanotube/Manganese Oxide Ultrathin Film Electrodes for Electrochemical Capacitors. *ACS Nano* **2010**, *4*, 3889–3896. [CrossRef]
9. Gogotsi, Y.; Simon, P. True Performance Metrics in Electrochemical Energy Storage. *Science* **2011**, *334*, 917–918. [CrossRef]
10. Simon, P.; Gogotsi, Y. Materials for electrochemical capacitors. *Nanosci. Technol.* **2009**, 320–329. [CrossRef]
11. Lee, C.Y.; Tsai, H.M.; Chuang, H.J.; Li, S.Y.; Lin, P.; Tseng, T.Y. Characteristics and electrochemical performance of supercapacitors with manganese oxide-carbon nanotube nanocomposite electrodes. *J. Electrochem. Soc.* **2005**, *152*, A716. [CrossRef]
12. Grover, S.; Shekhar, S.; Sharma, R.K.; Singh, G. Multiwalled carbon nanotube supported polypyrrole manganese oxide composite supercapacitor electrode: Role of manganese oxide dispersion in performance evolution. *Electrochim. Acta* **2014**, *116*, 137–145. [CrossRef]
13. Dong, X.; Shen, W.; Gu, J.; Xiong, L.; Zhu, Y.; Li, A.H.; Shi, J. MnO_2-Embedded-in-Mesoporous-Carbon-Wall Structure for Use as Electrochemical Capacitors. *J. Phys. Chem. B* **2006**, *110*, 6015–6019. [CrossRef] [PubMed]
14. Raymundo-Pinero, E.; Khomenko, V.; Frackowiak, E.; Beguin, F. Performance of manganese oxide/CNTs composites as elec-trode materials for electrochemical capacitors. *J. Electrochem. Soc.* **2004**, *152*, A229. [CrossRef]
15. Che, G.; Lakshmi, B.B.; Martin, C.R.; Fisher, E.R. Metal-Nanocluster-Filled Carbon Nanotubes: Catalytic Properties and Possible Applications in Electrochemical Energy Storage and Production. *Langmuir* **1999**, *15*, 750–758. [CrossRef]
16. Das, R.K.; Liu, B.; Reynolds, J.R.; Rinzler, A.G. Engineered Macroporosity in Single-Wall Carbon Nanotube Films. *Nano Lett.* **2009**, *9*, 677–683. [CrossRef]
17. Deng, X.; Bai, X.; Cai, Z.; Huang, M.; Chen, X.; Huang, B.; Chen, Y. Renewable carbon foam/δ-MnO_2 composites with well-defined hierarchical microstructure as supercapacitor electrodes. *J. Mater. Res. Technol.* **2020**, *9*, 8544–8555. [CrossRef]
18. Xiong, C.; Li, M.; Zhao, W.; Duan, C.; Ni, Y. Flexible N-doped reduced graphene oxide/carbon nanotube-MnO_2 film as a multifunctional material for high-performance supercapacitors, catalysts and sensors. *J. Mater.* **2020**, *6*, 523–531.
19. Wen, J.; Chen, X.; Huang, M.; Yang, W.; Deng, J. Core–shell-structured MnO_2@carbon spheres and nitrogen-doped activated carbon for asymmetric supercapacitors with enhanced energy density. *J. Chem. Sci.* **2020**, *132*, 1–11. [CrossRef]
20. Wang, J.; Guo, X.; Cui, R.; Huang, H.; Liu, B.; Li, Y.; Sun, B. MnO_2/Porous Carbon Nanotube/MnO_2 Nanocomposites for High-Performance Supercapacitor. *ACS Appl. Nano Mater.* **2020**, *3*, 11152–11159. [CrossRef]
21. Hu, Y.; Wu, Y.; Wang, J. Manganese-Oxide-Based Electrode Materials for Energy Storage Applications: How Close Are We to the Theoretical Capacitance? *Adv. Mater.* **2018**, *30*, e1802569. [CrossRef]
22. Li, H.; Wang, R.; Cao, R. Physical and electrochemical characterization of hydrous ruthenium oxide/ordered mesoporous carbon composites as supercapacitor. *Microporous Mesoporous Mater.* **2008**, *111*, 32–38. [CrossRef]
23. Kim, H.; Popov, B.N. Characterization of hydrous ruthenium oxide/carbon nanocomposite supercapacitors prepared by a colloidal method. *J. Power Sources* **2002**, *104*, 52–61. [CrossRef]
24. Ye, J.-S.; Cui, H.F.; Liu, X.; Lim, T.M.; Zhang, W.-D.; Sheu, F.-S. Preparation and Characterization of Aligned Carbon Nanotube-Ruthenium Oxide Nanocomposites for Supercapacitors. *Small* **2005**, *1*, 560–565. [CrossRef]
25. Yuan, C.; Chen, L.; Gao, B.; Su, L.; Zhang, X. Synthesis and utilization of $RuO_2 \cdot xH_2O$ nanodots well dispersed on poly(sodium 4-styrene sulfonate) functionalized multi-walled carbon nanotubes for supercapacitors. *J. Mater. Chem.* **2008**, *19*, 246–252. [CrossRef]
26. Yang, L.; Zhang, J.; Zhang, Y.; Zhao, Y.; Yin, H.; Hua, Q.; Yuan, J.; Tang, J. A ternary composite RuO_2@SWCNT/graphene for high performance electrochemical capacitors. *Mater. Lett.* **2020**, *259*, 126860. [CrossRef]
27. Chen, L.Y.; Hou, Y.; Kang, J.L.; Hirata, A.; Fujita, T.; Chen, M. Toward the Theoretical Capacitance of RuO_2Reinforced by Highly Conductive Nanoporous Gold. *Adv. Energy Mater.* **2013**, *3*, 851–856. [CrossRef]
28. Soudan, P.; Gaudet, J.; Guay, D.; Bélanger, D.; Schulz, R. Electrochemical Properties of Ruthenium-Based Nanocrystalline Materials as Electrodes for Supercapacitors. *Chem. Mater.* **2002**, *14*, 1210–1215. [CrossRef]
29. Lee, H.Y.; Goodenough, J.B. Supercapacitor Behavior with KCl Electrolyte. *J. Solid State Chem.* **1999**, *144*, 220–223. [CrossRef]
30. Wei, W.; Cui, X.; Chen, W.; Ivey, D.G. Phase-controlled synthesis of MnO_2 nanocrystals by anodic electrodeposition: Implica-tions for high-rate capability electrochemical supercapacitors. *J. Phys. Chem. C* **2008**, *112*, 15075–15083. [CrossRef]
31. Munoz-Paez, A. Transition Metal Oxides: Geometric and Electronic Structures: Introducing Solid State Topics in Inorganic Chemistry Courses. *J. Chem. Educ.* **1994**, *71*, 381–388. [CrossRef]
32. Toupin, M.; Brousse, T.; Bélanger, D. Influence of Microstucture on the Charge Storage Properties of Chemically Synthesized Manganese Dioxide. *Chem. Mater.* **2002**, *14*, 3946–3952. [CrossRef]
33. Hu, C.C.; Tsou, T.W. Ideal capacitive behavior of hydrous manganese oxide prepared by anodic deposition. *Electrochem. Commun.* **2002**, *4*, 105–109. [CrossRef]
34. Huang, M.; Li, F.; Dong, F.; Zhang, Y.X.; Zhang, L.L. MnO_2-based nanostructures for high-performance supercapacitors. *J. Mater. Chem. A* **2015**, *3*, 21380–21423. [CrossRef]

35. Qiu, Y.; Xu, P.; Guo, B.; Cheng, Z.; Fan, H.; Yang, M.; Yang, X.; Li, J. Electrodeposition of manganese dioxide film on activated carbon paper and its application in supercapacitors with high rate capability. *RSC Adv.* **2014**, *4*, 64187–64192. [CrossRef]
36. Hu, Y.; Wang, J. MnOx nanosheets for improved electrochemical performances through bilayer nano-architecting. *J. Power Sources* **2015**, *286*, 394–399. [CrossRef]
37. Tang, X.; Liu, Z.-H.; Zhang, C.; Yang, Z.; Wang, Z. Synthesis and capacitive property of hierarchical hollow manganese oxide nanospheres with large specific surface area. *J. Power Sources* **2009**, *193*, 939–943. [CrossRef]
38. Li, W.; Xu, K.; Li, B.; Sun, J.; Jiang, F.; Yu, Z.; Zou, R.; Chen, Z.; Hu, J. Cover Picture: MnO_2 Nanoflower Arrays with High Rate Capability for Flexible Supercapacitors (ChemElectroChem 6/2014). *ChemElectroChem* **2014**, *1*, 960. [CrossRef]
39. Yang, P.; Ding, Y.; Lin, Z.; Chen, Z.; Li, Y.; Qiang, P.; Ebrahimi, M.; Mai, W.; Wong, C.P.; Wang, Z.L. Low-Cost High-Performance Solid-State Asymmetric Supercapacitors Based on MnO_2 Nanowires and Fe_2O_3 Nanotubes. *Nano Lett.* **2014**, *14*, 731–736. [CrossRef]
40. Ma, S.-B.; Ahn, K.-Y.; Lee, E.-S.; Oh, K.-H.; Kim, K.-B. Synthesis and characterization of manganese dioxide spontaneously coated on carbon nanotubes. *Carbon* **2007**, *45*, 375–382. [CrossRef]
41. Kim, G.; Ryu, I.; Yim, S. Retarded saturation of the areal capacitance using 3D-aligned MnO_2 thin film nanostructures as a supercapacitor electrode. *Sci. Rep.* **2017**, *7*, 1–9. [CrossRef]
42. Wang, G.; Xu, H.; Lu, L.; Zhao, H. One-step synthesis of mesoporous MnO_2/carbon sphere composites for asymmetric electrochemical capacitors. *J. Mater. Chem. A* **2015**, *3*, 1127–1132. [CrossRef]
43. El-Kady, M.F.; Ihns, M.; Li, M.; Hwang, J.Y.; Mousavi, M.F.; Chaney, L.; Lech, A.T.; Kaner, R.B. Engineering three-dimensional hybrid supercapacitors and microsupercapacitors for high-performance integrated energy storage. *Proc. Natl. Acad. Sci. USA* **2015**, *112*, 4233–4238. [CrossRef]
44. Wei, W.; Cui, X.; Chen, W.; Ivey, D.G. Manganese oxide-based materials as electrochemical supercapacitor electrodes. *Chem. Soc. Rev.* **2010**, *40*, 1697–1721. [CrossRef]
45. Chang, H.-W.; Jeng-Lung, C.; Chen, J.-L.; Chen, C.-L.; Lee, J.-F.; Chen, J.-M.; Tsai, Y.-C.; Chang, C.-M.; Yeh, P.-H.; Chou, W.-C.; et al. Nanoflaky MnO_2/functionalized carbon nanotubes for supercapacitors: An in situ X-ray absorption spectroscopic investigation. *Nanoscale* **2015**, *7*, 1725–1735. [CrossRef] [PubMed]
46. De Oliveira, A.H.P.; Nascimento, M.L.F.; de Oliveira, H.P. Carbon nanotube@MnO_2@ polypyrrole composites: Chemical synthesis, characterization and application in supercapacitors. *Mater. Res.* **2016**, *19*, 1080–1087. [CrossRef]
47. Bai, Z.; Li, H.; Li, M.; Li, C.; Wang, X.; Qu, C.; Yang, B. Flexible carbon nanotubes-MnO_2/reduced graphene oxide-polyvinylidene fluoride films for supercapacitor electrodes. *Int. J. Hydrogen Energy* **2015**, *40*, 16306–16315. [CrossRef]
48. Xiong, T.; Lee, W.S.V.; Huang, X.; Xue, J.M. Mn_3O_4/reduced graphene oxide based supercapacitor with ultra-long cycling performance. *J. Mater. Chem. A* **2017**, *5*, 12762–12768. [CrossRef]
49. Peigney, A.; Laurent, C.; Flahaut, E.; Bacsa, R.; Rousset, A. Specific surface area of carbon nanotubes and bundles of carbon nanotubes. *Carbon* **2001**, *39*, 507–514. [CrossRef]
50. Bacsa, R.; Laurent, C.; Peigney, A.; Bacsa, W.; Vaugien, T.; Rousset, A. High specific surface area carbon nanotubes from catalytic chemical vapor deposition process. *Chem. Phys. Lett.* **2000**, *323*, 566–571. [CrossRef]
51. Wang, J.W.; Chen, Y.; Chen, B.Z. A synthesis method of MnO_2/activated carbon composite for electrochemical supercapacitors. *J. Electrochem. Soc.* **2015**, *162*, A1654. [CrossRef]
52. Zhi, M.; Xiang, C.; Li, J.; Li, M.; Wu, N. Nanostructured carbon–metal oxide composite electrodes for supercapacitors: A review. *Nanoscale* **2013**, *5*, 72–88. [CrossRef] [PubMed]
53. Jang, Y.; Jo, J.; Jang, H.; Kim, I.; Kang, D.; Kim, K.Y. Activated carbon/manganese dioxide hybrid electrodes for high performance thin film supercapacitors. *Appl. Phys. Lett.* **2014**, *104*, 243901. [CrossRef]
54. Xu, L.; Jia, M.; Li, Y.; Jin, X.; Zhang, F. High-performance MnO_2-deposited graphene/activated carbon film electrodes for flexible solid-state supercapacitor. *Sci. Rep.* **2017**, *7*, 12857. [CrossRef] [PubMed]
55. Cheng, Z.; Tan, G.; Qiu, Y.; Guo, B.; Cheng, F.; Fan, H. High performance electrochemical capacitors based on MnO_2/activated-carbon-paper. *J. Mater. Chem. C* **2015**, *3*, 6166–6171. [CrossRef]
56. Iijima, S. Helical microtubules of graphitic carbon. *Nat. Cell Biol.* **1991**, *354*, 56–58. [CrossRef]
57. Moon, Y.S.; Kim, D.; Lee, G.; Hong, S.Y.; Kim, K.K.; Park, S.M.; Ha, J.S. Fabrication of flexible micro-supercapacitor array with patterned graphene foam/MWNT-COOH/MnOx electrodes and its application. *Carbon* **2015**, *81*, 29–37. [CrossRef]
58. Zhang, Z.; Xiao, F.; Wang, S. Hierarchically structured MnO_2/graphene/carbon fiber and porous graphene hydrogel wrapped copper wire for fiber-based flexible all-solid-state asymmetric supercapacitors. *J. Mater. Chem. A* **2015**, *3*, 11215–11223. [CrossRef]
59. Zhang, X.; Shi, W.; Zhu, J.; Kharistal, D.J.; Zhao, W.; Lalia, B.S.; Hng, H.H.; Yan, Q. High-Power and High-Energy-Density Flexible Pseudocapacitor Electrodes Made from Porous CuO Nanobelts and Single-Walled Carbon Nanotubes. *ACS Nano* **2011**, *5*, 2013–2019. [CrossRef]
60. Hou, Y.; Cheng, Y.; Hobson, T.; Liu, J. Design and synthesis of hierarchical MnO_2 nanospheres/carbon nanotubes/conducting polymer ternary composite for high performance electrochemical electrodes. *Nano Lett.* **2010**, *10*, 2727–2733. [CrossRef]
61. Chen, H.; Zeng, S.; Chen, M.; Zhang, Y.; Zheng, L.; Li, Q. Oxygen Evolution Assisted Fabrication of Highly Loaded Carbon Nanotube/MnO_2 Hybrid Films for High-Performance Flexible Pseudosupercapacitors. *Small* **2016**, *12*, 2035–2045. [CrossRef] [PubMed]

62. Yeo, T.; Shin, D.; Shin, J.; Hwang, H.; Seo, B.; Lee, J.; Choi, W. DC-field-driven combustion waves for one-step fabrication of reduced manganese oxide/multi-walled carbon nanotube hybrid nanostructures as high-performance supercapacitor elec-trodes. *J. Mater. Chem. A* **2017**, *5*, 24707–24719. [CrossRef]
63. Huang, G.; Zhang, Y.; Wang, L.; Sheng, P.; Peng, H. Fiber-based MnO_2/carbon nanotube/polyimide asymmetric supercapacitor. *Carbon* **2017**, *125*, 595–604. [CrossRef]
64. Wang, L.; Huang, M.; Chen, S.; Kang, L.; He, X.; Lei, Z.; Shi, F.; Xu, H.; Liu, Z.H. δ-MnO_2 nanofiber/single-walled carbon nanotube hybrid film for all-solid-state flexible supercapacitors with high performance. *J. Mater. Chem. A* **2017**, *5*, 19107–19115. [CrossRef]
65. Shi, P.; Li, L.; Hua, L.; Qian, Q.; Wang, P.; Zhou, J.; Sun, G.; Huang, W. Design of Amorphous Manganese Oxide@Multiwalled Carbon Nanotube Fiber for Robust Solid-State Supercapacitor. *ACS Nano* **2017**, *11*, 444–452. [CrossRef]
66. Li, P.; Yang, Y.; Shi, E.; Shen, Q.; Shang, Y.; Wu, S.; Wei, J.; Wang, K.; Zhu, H.; Yuan, Q.; et al. Core-double-shell, carbon nanotube@ polypyrrole@ MnO_2 sponge as freestanding, compressible supercapacitor electrode. *ACS Appl. Mater. Interfaces* **2014**, *6*, 5228–5234. [CrossRef] [PubMed]
67. Higgins, T.M.; McAteer, D.; Coelho, J.C.M.; Sanchez, B.M.; Gholamvand, Z.; Moriarty, G.; McEvoy, N.; Berner, N.C.; Duesberg, G.S.; Nicolosi, V.; et al. Effect of Percolation on the Capacitance of Supercapacitor Electrodes Prepared from Composites of Manganese Dioxide Nanoplatelets and Carbon Nanotubes. *ACS Nano* **2014**, *8*, 9567–9579. [CrossRef]
68. Jin, Y.; Chen, H.; Chen, M.; Liu, N.; Li, Q. Graphene-Patched CNT/MnO_2 Nanocomposite Papers for the Electrode of High-Performance Flexible Asymmetric Supercapacitors. *ACS Appl. Mater. Interfaces* **2013**, *5*, 3408–3416. [CrossRef]
69. Cheng, Y.; Zhang, H.; Lu, S.; Varanasi, C.V.; Liu, J. Flexible asymmetric supercapacitors with high energy and high power density in aqueous electrolytes. *Nanoscale* **2013**, *5*, 1067–1073. [CrossRef]
70. Amade, R.; Jover, E.; Caglar, B.; Mutlu, T.; Bertran, E. Optimization of MnO_2/vertically aligned carbon nanotube composite for supercapacitor application. *J. Power Sources* **2011**, *196*, 5779–5783. [CrossRef]
71. Qian, J.; Jin, H.; Chen, B.; Lin, M.; Lu, W.; Tang, W.M.; Xiong, W.; Chan, L.W.H.; Lau, S.P.; Yuan, J. Aqueous Manganese Dioxide Ink for Paper-Based Capacitive Energy Storage Devices. *Angew. Chem. Int. Ed.* **2015**, *54*, 6800–6803. [CrossRef]
72. Liu, J.; Li, F.; Li, X.; He, X. Ultrathin MnO_2 nanosheets grown on hollow carbon spheres with enhanced capacitive performance. *Phys. Lett. A* **2020**, *384*, 126539. [CrossRef]
73. Zhang, C.; Hatzell, K.B.; Boota, M.; Dyatkin, B.; Beidaghi, M.; Long, D.; Qiao, W.; Kumbur, E.C.; Gogotsi, Y. Highly porous carbon spheres for electrochemical capacitors and capacitive flowable suspension electrodes. *Carbon* **2014**, *77*, 155–164. [CrossRef]
74. Zhao, Y.; Meng, Y.; Jiang, P. Carbon@MnO_2 core–shell nanospheres for flexible high-performance supercapacitor electrode materials. *J. Power Sources* **2014**, *259*, 219–226. [CrossRef]
75. Yang, Z.-C.; Tang, C.-H.; Gong, H.; Li, X.; Wang, J. Hollow spheres of nanocarbon and their manganese dioxide hybrids derived from soft template for supercapacitor application. *J. Power Sources* **2013**, *240*, 713–720. [CrossRef]
76. Xiong, Y.; Zhou, M.; Chen, H.; Feng, L.; Wang, Z.; Yan, X.; Guan, S. Synthesis of honeycomb MnO_2 nanospheres/carbon na-noparticles/graphene composites as electrode materials for supercapacitors. *Appl. Surf. Sci.* **2015**, *357*, 1024–1030. [CrossRef]
77. Ranjusha, R.; Ramakrishna, S.; Nair, A.S.; Anjali, P.; Vineeth, S.; Sonia, T.S.; Sivakumar, N.; Subramanian, K.R.V.; Nair, S.V.; Balakrishnan, A. Fabrication and performance evaluation of button cell supercapacitors based on MnO_2 nanowire/carbon nanobead electrodes. *RSC Adv.* **2013**, *3*, 17492–17499. [CrossRef]
78. Frackowiak, E.; Béguin, F. Carbon materials for the electrochemical storage of energy in capacitors. *Carbon* **2001**, *39*, 937–950. [CrossRef]
79. Yuan, L.; Lu, X.H.; Xiao, X.; Zhai, T.; Dai, J.; Zhang, F.; Hu, B.; Wang, X.; Gong, L.; Chen, J.; et al. Flexible solid-state supercapacitors based on carbon nanoparticles/MnO_2 nanorods hybrid structure. *ACS Nano* **2012**, *6*, 656–661. [CrossRef]
80. Choi, C.; Kim, S.H.; Sim, H.J.; Lee, J.A.; Choi, A.Y.; Kim, Y.T.; Lepro, X.; Spinks, G.M.; Baughman, R.H.; Kim, S.J. Stretchable, Weavable Coiled Carbon Nanotube/MnO_2/Polymer Fiber Solid-State Supercapacitors. *Sci. Rep.* **2015**, *5*, 9387. [CrossRef]
81. Wang, J.-G.; Yang, Y.; Huang, Z.-H.; Kang, F. A high-performance asymmetric supercapacitor based on carbon and carbon–MnO_2 nanofiber electrodes. *Carbon* **2013**, *61*, 190–199. [CrossRef]
82. Bao, L.; Zang, J.; Li, X. Flexible Zn_2SnO_4/MnO_2 core/shell nanocable− carbon microfiber hybrid composites for high-performance supercapacitor electrodes. *Nano Lett.* **2011**, *11*, 1215–1220. [CrossRef]
83. Xu, H.; Hu, X.; Yang, H.; Sun, Y.; Hu, C.; Huang, Y. Flexible Asymmetric Micro-Supercapacitors Based on $Bi_2O_3$and MnO_2 Nanoflowers: Larger Areal Mass Promises Higher Energy Density. *Adv. Energy Mater.* **2015**, *5*, 1401882. [CrossRef]
84. Chen, Y.; Qin, W.-Q.; Wang, J.-W.; Chen, B.-Z. Fabrication and electrochemical performance of nanoflake MnO_2@carbon fiber coaxial nanocables for supercapacitors. *J. Appl. Electrochem.* **2016**, *46*, 241–249. [CrossRef]
85. Dang, W.; Dong, C.; Zhang, Z.; Chen, G.; Wang, Y.; Guan, H. Self-grown MnO_2 nanosheets on carbon fiber paper as high-performance supercapacitors electrodes. *Electrochim. Acta* **2016**, *217*, 16–23. [CrossRef]
86. Yang, Q.; Dong, L.; Xu, C.; Kang, F. High-performance supercapacitors based on graphene/MnO_2/activated carbon fiber felt composite electrodes in different neutral electrolytes. *RSC Adv.* **2016**, *6*, 12525–12529. [CrossRef]
87. Ramezani, M.; Fathi, M.; Mahboubi, F. Facile synthesis of ternary MnO_2/graphene nanosheets/carbon nanotubes composites with high rate capability for supercapacitor applications. *Electrochim. Acta* **2015**, *174*, 345–355. [CrossRef]
88. Zhang, G.; Ren, L.; Deng, L.; Wang, J.; Kang, L.; Liu, Z.-H. Graphene–MnO_2 nanocomposite for high-performance asymmetrical electrochemical capacitor. *Mater. Res. Bull.* **2014**, *49*, 577–583. [CrossRef]

89. Zhou, H.; Yang, X.; Lv, J.; Dang, Q.; Kang, L.; Lei, Z.; Yang, Z.; Hao, Z.; Liu, Z.-H. Graphene/MnO_2 hybrid film with high capacitive performance. *Electrochim. Acta* **2015**, *154*, 300–307. [CrossRef]
90. Mahmood, M.; Rasheed, A.; Ayman, I.; Rasheed, T.; Munir, S.; Ajmal, S.; Agboola, P.O.; Warsi, M.F.; Shahid, M. Synthesis of Ultrathin MnO_2 Nanowire-Intercalated 2D-MXenes for High-Performance Hybrid Supercapacitors. *Energy Fuels* **2021**, *35*, 3469–3478. [CrossRef]
91. Ma, Z.; Fan, L.; Jing, F.; Zhao, J.; Liu, Z.; Li, Q.; Li, J.; Fan, Y.; Dong, H.; Qin, X.; et al. MnO_2 Nanowires@NiCo-LDH Nanosheet Core–Shell Heterostructure: A Slow Irreversible Transition of Hydrotalcite Phase for High-Performance Pseudocapacitance Electrode. *ACS Appl. Energy Mater.* **2021**. [CrossRef]
92. Sun, X.; Wang, J.; Chen, B.; Dai, G.; Situ, Y.; Huang, H. High-performance adjustable manganese oxides hybrid nanostructure for supercapacitors. *Electrochim. Acta* **2021**, *381*, 138213. [CrossRef]
93. Zhang, K.; Han, X.; Hu, Z.; Zhang, X.; Tao, Z.; Chen, J. Nanostructured Mn-based oxides for electrochemical energy storage and conversion. *Chem. Soc. Rev.* **2015**, *44*, 699–728. [CrossRef] [PubMed]